Research, Society and Development, v. 10, n. 10, e326101019028, 2021
(CC BY 4.0) | ISSN 2525-3409 | DOI: http://dx.doi.org/10.33448/rsd-v10i10.19028

Determination of thickness and refractive index of SiO_2 thin films using the cross-entropy global optimization method

Determinação da espessura e índice de refração de filmes finos de SiO_2 usando o método de otimização global Cross-entropy

Determinación del espesor y el índice de refracción de películas delgadas de SiO_2 utilizando el método de optimización global Cross-entropy

Received: 07/03/2021 | Reviewed: 08/07/2021 | Accept: 08/07/2021 | Published: 08/14/2021

Sávio José Vieira Zaccaro
ORCID: https://orcid.org/0000-0001-7852-4689
Universidade Federal de Itajubá, Brazil
E-mail: savio.v.z@gmail.com
Adhimar Flávio Oliveira
ORCID: https://orcid.org/0000-0003-2586-7359
Universidade Federal de Itajubá, Brazil
E-mail: adhimarflavio@unifei.edu.br
Rero Marques Rubinger
ORCID: https://orcid.org/0000-0003-1718-9658
Universidade Federal de Itajubá, Brazil
E-mail: rero@unifei.edu.br
Crediana Chris de Siqueira
ORCID: https://orcid.org/0000-0001-8922-4972
Universidade Federal de Itajubá, Brazil
E-mail: d2017012305@unifei.edu.br
Roberto Affonso da Costa Junior
Universidade Federal de Itajubá, Brazil
E-mail: rcosta62br@unifei.edu.br
"In memoriam"

Abstract
Silicon dioxide (SiO_2) is a material that is abundant in nature and has wide application in semiconductor and insulating devices. In this work, a set of six SiO_2 samples were grown on a Sigma-Aldrich Silicon substrate, varying the growth time and temperature. This set of samples were grown using times of 10 and 12h and temperatures of 800, 900, and 1000 ºC, under ambient atmosphere. After film growth, reflectance measurements were performed on the films and the substrate, using the Stellarnet UV-VIS-NIR spectrophotometer between 194 and 1081.5 nm. These measurements were modeled using a global optimization method, called Cross-entropy, together with the Bootstrapping resampling technique, seeking to robustly and statistically determine the thin film refractive index as a function of the wavelength and its thickness. To estimate the refractive index of the SiO_2 thin film, the Cauchy model was used. For the substrate, reflectance measurements were used. The method proved to be efficient, presenting thickness values that were validated according to growth parameters and literature data. This method proved to be an important and low-cost tool, compared to traditional methods, to help in the steps of building thin films for semiconductor and insulating devices, thus improving their physical properties and enabling the development of new devices.
Keywords: Global optimization; Optical characterization; Thin film; Cauchy model; SiO_2; Cross-entropy; Bootstrapping.

Resumo
O dióxido de silício (SiO2) é um material abundante na natureza e que possui ampla aplicação em dispositivos semicondutores e isolantes. Neste trabalho foi realizado o crescimento de um conjunto de seis amostras de SiO_2 em substrato de Silício Sigma-Aldrich, variando o tempo e a temperatura de crescimento. Este conjunto de amostras foram crescidas utilizando tempos de 10 e 12h e temperaturas de 800, 900 e 1000 ºC, sobre atmosfera ambiente. Após o crescimento dos filmes, realizou-se medidas de refletância nos filmes eno substrato, utilizando o espectrofotômetro Stellarnet UV-VIS-NIR entre 194 a 1081,5 nm. Estas medidas foram modeladas utilizando um método de otimização global, nomeado Cross-entropy, juntamente com a técnica de reamostragem Bootstrapping, buscando determinar de forma robusta e estatística o índice de refração do filme fino em função do comprimento de onda e sua espessura. Para estimar o índice de refração do filme fino de SiO_2 foi utilizado o modelo de Cauchy. Para o substrato foram utilizadas as medidas de refletância. O método se mostrou eficiente, apresentando valores de espessura que foram validados de

acordo com os parâmetros de crescimento e dados da literatura. Tal método se mostrou uma ferramenta importante e de baixo custo, em comparação com os métodos tradicionais, para ajudar nas etapas de construção de filmes finos para dispositivos semicondutores e isolantes, melhorando assim, suas propriedades físicas e também possibilitando o desenvolvimento de novos dispositivos.
Palavras-chave: Otimização global; Caracterização óptica; Filme fino; Modelo de Cauchy; SiO_2; Cross-entropy; Bootstrapping.

Resumen
El dióxido de silicio (SiO_2) es un material abundante en la naturaleza y tiene una amplia aplicación en dispositivos semiconductores y aislantes. En este trabajo, se cultivó un conjunto de seis muestras de SiO_2 en un sustrato de silicio Sigma-Aldrich, variando el tiempo de crecimiento y la temperatura. Este conjunto de muestras se cultivó utilizando tiempos de 10 y 12 h y temperaturas de 800, 900 y 1000 ° C, en atmósfera ambiente. Después del crecimiento de la película, se realizaron mediciones de reflectancia en las películas y en el sustrato, utilizando el espectrofotómetro Stellarnet UV-VIS-NIR entre 194 y 1081,5 nm. Estas medidas se modelaron utilizando un método de optimización global, llamado Cross-entropía, junto con la técnica de remuestreo Bootstrapping, buscando determinar de manera robusta y estadísticamente el índice de refracción de película delgada en función de la longitud de onda y su espesor. Para estimar el índice de refracción de la película delgada de SiO_2, se utilizó el modelo de Cauchy. Para el sustrato, se utilizaron medidas de reflectancia. El método demostró ser eficiente, presentando valores de espesor que fueron validados según parámetros de crecimiento y datos de la literatura. Este método demostró ser una herramienta importante y de bajo costo, en comparación con los métodos tradicionales, para ayudar en los pasos de construcción de películas delgadas para dispositivos semiconductores y aislantes, mejorando así sus propiedades físicas y permitiendo el desarrollo de nuevos dispositivos.
Palabras clave: Optimización global; Caracterización óptica; Película delgada; Modelo de Cauchy; SiO_2; Cross-entropy; Bootstrapping.

1. Introduction

SiO_2 is a transparent, crystalline, and odorless material belonging to the group of metallic oxides, it is one of the most abundant compounds on the planet; it has been used for a long time and is present in various forms to this day. The Romans since that time already used silicon dioxide in the form of sand in concrete to improve its resistance properties, also using SiO_2 in the form of quartz gemstone jewelry. Wristwatches also use quartz to increase time accuracy, and quartz has piezoelectric properties and can be used in transducers. Glass is another example of the variation of this material, it is widely used and also consists mainly of silicon dioxide, along with other compounds (Zou et al. 2019, Black et al. 1988).

Currently, modern electronics depend on SiO_2, for example in the manufacture of optical fibers, MOS technology, and semiconductors as well as silicon, which can be manufactured from silicon dioxide, and these are also applied in transistors, diodes, etc (Vidakis et al. 2021, El-Bindary et al. 2021).

Another form of application is through thin films, these play an essential role in devices and integrated circuits (Curran et al. 2021, Chakravarty et al. 2021). They are used in the connections of active regions of a device, in communication between devices, in external access to circuits, to isolate conductive layers, as structural elements of devices, to protect surfaces from the external environment, as a source of dopant and as a barrier to the doping.

Determining thin film parameters such as refractive index and thickness is of great importance in the production of devices that use optical interference (Gao et al. 2013). The quality of manufactured devices directly depends on the accuracy of these parameters. The reflectance of the film can vary with the variation of the refractive index, the refractive index value is used to assess the quality of the grown film: greater than 1.46 indicates a silicon-rich film, while smaller indicates a low-density porous film. The optical thickness parameters are normally determined by the ellipsometry technique (Garcia-Caurel et al. 2013, Losurdo et al. 2009), but due to the high cost and complexity, a low-cost alternative was sought. Using non-destructive reflectance measurements through a UV-VIS-NIR spectrometer and then modeling the data with theoretical predictions that depend on the refractive indices belonging to the air/film/substrate set and the film thickness (Rubinger et al. 2015, Jesus et al. 2021). Thus, we present the results of modeling reflectance measurements using the cross-entropy (CE) global optimization method (Oliveira et al. 2016, Ribeiro et al. 2021) and discuss the results obtained for a homogeneous SiO_2 film and its respective

refractive index under different oxidation conditions. This being an experimental research that the methodology presented in Pereira et al. (2018)

2. Refractive Index

The refractive index *n* in an optical or dielectric medium is the ratio of the speed of light *c* in a vacuum to the speed *v* in the medium, *n=c/v*. Using this and Maxwell's equations, we obtain the para ratio of the refractive index for a substance $n = \sqrt{\varepsilon\mu}$, where ε is the permittivity and μ the magnetic permeability (Batsanov et al. 2016). For non-magnetic substances, we can write $n = \sqrt{\varepsilon}$, which is very useful for relating the dielectric properties of a material to its optical properties, at any specific frequency of interest. Since ε depends on the wavelength of light, the index of refraction also depends, which is called scattering. In addition to dispersion, an electromagnetic wave also suffers energy losses through mechanisms such as phonon generation, photogeneration, absorption by carriers, and scattering. In such materials, the refractive index is a complex function of frequency.

The complex index of refraction *N*, with real part *n* and imaginary part *k*, which is called extinction coefficient, is related to the complex permissiveness, $\varepsilon = \varepsilon' - i\varepsilon''$for

$$N = n - ik = \sqrt{\varepsilon} = \sqrt{\varepsilon' - i\varepsilon''} \quad (1)$$

where ε' and ε'' are respectively the real and imaginary part of ε. Reflectance *R* is defined by

$$n^2 - k^2 = \varepsilon'$$

$$2nk = \varepsilon''$$

The optical constants *n* and *k* can be determined from the material surface reflectance as a function of polarization and incident angle. For a normal incidence, the reflection coefficient r is obtained by

$$r = \frac{1 - N}{1 + N} = \frac{1 - n + ik}{1 + n - ik} \quad (2)$$

and

$$R = |r^2| = \left|\frac{1 - n + ik}{1 + n - ik}\right|^2 = \frac{(1 - n)^2 + k^2}{(1 + n)^2 + k^2} \quad (3)$$

In the limit where $k = 0$, we can rewrite writing the index of refraction as a function of reflectance as follows

$$n = \frac{1 + R + 2\sqrt{R}}{1 - R} \quad (4)$$

This equation was used as an approximation for the refractive index of the silicon substrate, using the reflectance measurement performed in the laboratory.

To determine the refractive index of SiO_2, the Cauchy Equation (Li & Wu, 2004, Liu et al. 2019) was used. Cauchy wrote this equation in the year 1836 it accurately describes the dispersion of a transparent material as well as oxides. The equation is written as

$$n(\lambda) = A + \frac{B}{\lambda^2} + \frac{C}{\lambda^4} \quad (5)$$

In this equation, *A*, *B*, and *C* are constant coefficients characteristic of the material studied and λ the wavelength of light, in this case, values of λ compatible with those of the reflectance measurements made with the spectrometer were used, and the validity of your equation. In this work, the values of the coefficients *A*, *B*, and *C* were fitted simultaneously with the thin film thickness.

2.1 Three-layer model for thin films

This model is used to study films; it defines the reflectance of a film in the air/film/substrate set (Eckertová, 2012). The adjustment made is dependent on the refractive indices and the thickness d_1 of the material. Figure 1 illustrates the system, where, n_2 is the refractive index of air, n_1 is the refractive index of the film, and n_0 is the refractive index of the substrate and d_1 is the thickness of the thin film.

Figure 1: Model used to determine film thickness. In the illustration it is possible to verify the layers of air, film and substrate.

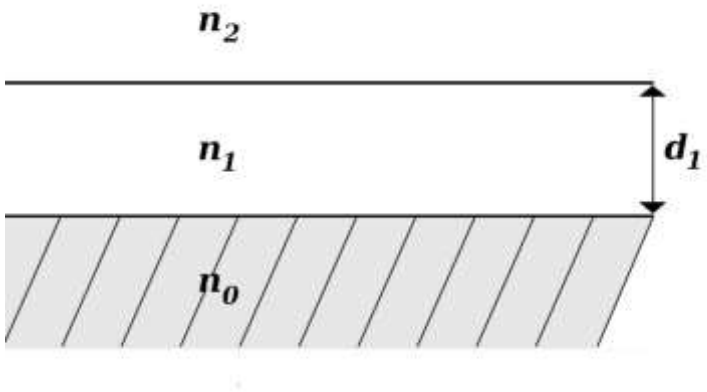

Source: Authors.

According to Heavens (Heavens, 1991), for a thin film considering that the means of interaction between radiation and matter is non-absorbent, the reflection coefficient is given by

$$R = \frac{r_2 + r_1 \exp(-2i\delta_1)}{1 + r_1 r_2 \exp(-2i\delta_1)} \quad (6)$$

where

$$\delta = 2\pi\nu n_1 d_1 \cos\phi \quad (7)$$

Since ϕ is the angle of incidence of the radiation as shown in Figure 2. In the assembly of the spectrometer, the incidence is normal to the surface, that is, $\phi = \pi/2$. The energy intensity per unit area per unit of time across the sample is given by

$$\mathbf{R} = RR^* = \frac{r_1{}^2 + 2r_1 r_2 \cos 2\delta_1 + r_2{}^2}{1 + 2r_1 r_2 \cos 2\delta_1 + r_1{}^2 r_2{}^2} \quad (8)$$

In the equation above, r_1 and r_2 are the Fresnel coefficients, and in this case, they are given by:

$$r_1 = \frac{n_1 - n_0}{n_1 + n_0} \quad (9)$$

$$r_2 = \frac{n_2 - n_1}{n_2 + n_1} \qquad (10)$$

Finally, the reflectance is rewritten as follows

$$\mathbf{R} = \frac{(n_0{}^2+n_1{}^2)(n_1{}^2+n_2{}^2)-4n_0\,n_1{}^2n_2+(n_0{}^2-n_1{}^2)(n_1{}^2-n_2{}^2)\cos\left(\frac{4\pi}{\lambda}n_1\,d_1\right)}{(n_0{}^2+n_1{}^2)(n_1{}^2+n_2{}^2)+4n_0\,n_1{}^2n_2+(n_0{}^2-n_1{}^2)(n_1{}^2-n_2{}^2)\cos\left(\frac{4\pi}{\lambda}n_1\,d_1\right)} \qquad (11)$$

Figure 2: Illustration of the behavior of radiation when crossing from one medium to another with different refractive index.

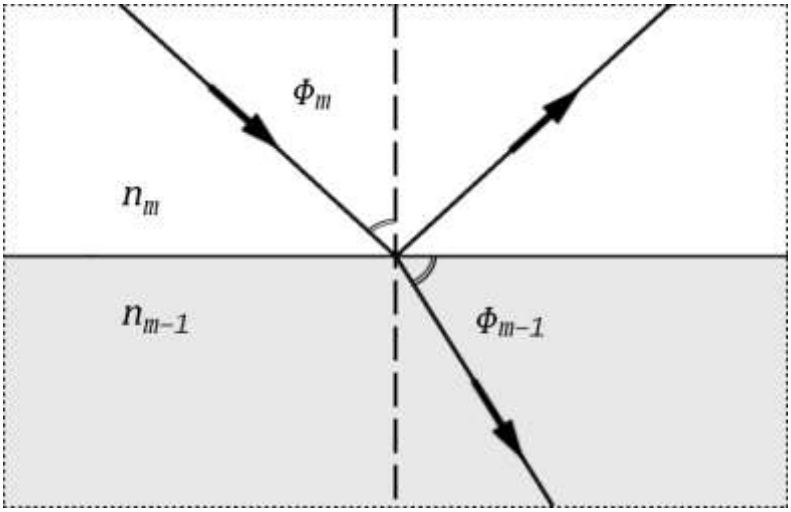

Source: Authors.

3. Methodology

The samples come from a Sigma-Aldrich brand silicon wafer that was divided into seven pieces of approximately 10 mm², using a diamond pen. Then, the samples went through the cleaning process, using acetone, isopropyl alcohol, and deionized water in an ultrasound bath, followed by drying in N_2. The samples were separately oxidized in an oven in the ambient atmosphere. The growth configurations of the samples were in a set with temperatures of 800, 900, and 1000ºC with a duration in the plateau of 10h and another set with the same temperatures, but with a duration in the plateau of 12h. Both the temperature and the oxidation time directly influence the thickness of the thin film grown, the higher the temperature and the dwell time at the temperature plateau, the greater the thickness of the film. The seventh remaining sample was used as a substrate reference for the reflectance adjustments.

On each oxidized sample and the substrate reference reflectance measurements were taken using a Stellarnet UV-VIS-NIR spectrometer and its accessories (Figure 3(a)) covering the wavelength range from 194 nm to 1081.5 nm, together with a halogen lamp whose characteristic spectrum is shown in Figure 3(b), in which an aluminum mirror was used as a reference.

Figure 3: (a) Stellarnet UV-VIS-NIR spectrometer and its accessories operating in reflectance mode. (b) The spectrum of the halogen lamp used for reflectance measurements.

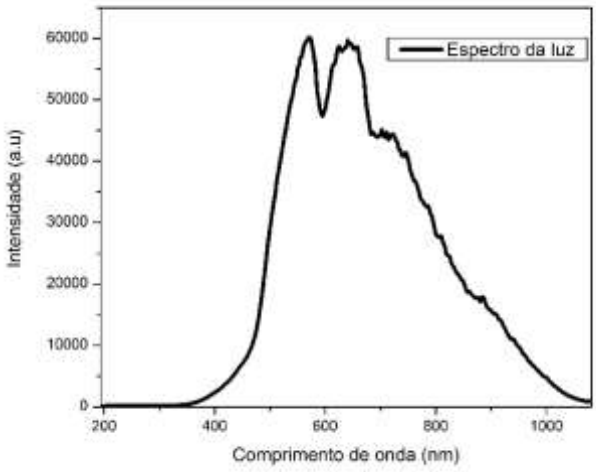

Source: Authors.

The reflectance measurement data were collected with the aid of Stellarnet Software. Before performing the measurement, the equipment was calibrated using a mirror with aluminum deposited by sputtering on the surface of the glass, one hundred percent light was defined for this mirror when the light source was turned on after this, it was turned off and the zero percent light. With the calibration parameters defined, the reflectance to the silicon substrate was measured, shown in Figure 4.

Figure 4: Reflectance measurement was performed for the Silicon substrate. This measure was used to determine the refractive index of the substratum of the sample.

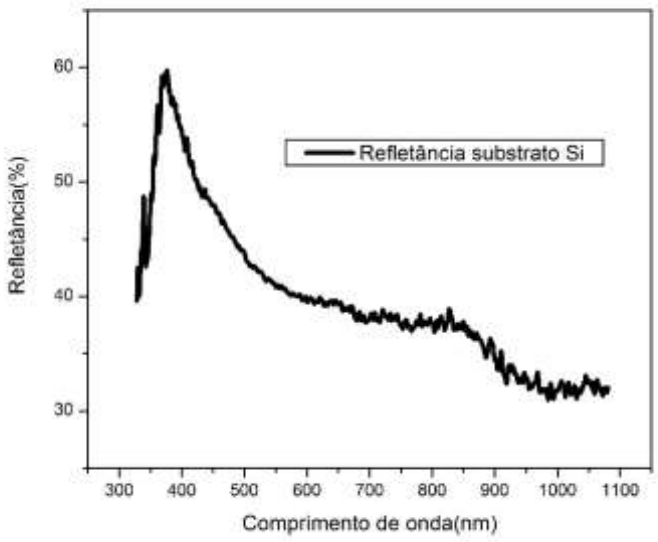

Source: Authors.

3.1 The Cross-Entropy Global Optimization Method

For data modeling, the CE global optimization method was used, which was first introduced by Rubinstein (Rubinstein, 1997), to estimate the probability of rare events in complex stochastic networks and soon after making some modifications to deal with continuous and discrete combinatorial optimization. CE has been used as an optimization method in several areas of knowledge, such as Astrophysics, Biology, Physics, Materials, and others (Oliveira et al. 2013, Rubinstein & Kroese, 2004), proving to be robust in problem-solving.

The CE uses sampling concepts, being a variance reduction technique, but it does not require prior knowledge of the parameters related to distribution. CE consists of a simple adaptive procedure for estimating parameters. Furthermore, the CE procedure is based on a solution space, with an evolutionary rule in which a fraction of the space is selected in each iteration based on some selection criteria.

To exemplify the functioning of the CE, consider a set of experimental data *x*, *y*, and *z* that can be modeled through a set of equations, whose parameters are *a*, *b*, and *c*, which are determined by the CE through the steps:

1. Random generation of an initial sample of parameters $= a_0, a_1, \ldots a_{i-1}$, $b = b_0, b_1, \ldots b_{i-1}$, and $c = c_0, c_1, \ldots c_{i-1}$ where i is the sample size, which must be defined initially. These values must obey a uniform distribution of probabilities and belong to an interval defined a priori, according to the model used.
2. Each set of parameters (a_i, b_i, c_i) is tested through an objective function and ranked in descending order from best fit to worst and a predefined percentage of the pairs is chosen.
3. From the parameters chosen in the previous step, a new improved sample of parameters is generated. Again, a normal probability distribution is used to generate a sample of parameters of the same size as the previous one, but in a smaller interval for the construction of sets. Note that the resolution of the set is a little higher. In addition, a mixing factor is assigned to the distribution so that the problem of the solution being parked at a local minimum does not occur.
4. The optimization process repeats steps 2 and 3 until a pre-defined stopping criterion is obtained.

Once convergence occurs, the set of parameters sought is obtained. In addition to the adjustment procedure, resampling of the data is performed using the technique called bootstrap (Zhu 1997, Jain et al. 1987, Boos 2003). This makes the procedure more robust, the fit is performed 1000 times with different sample sets of experimental data. On each repetition, some data is randomly removed and others inserted more than once.

In this work, the technique bootstrap and the global optimization method CE were applied, together with the experimental data of reflectance in the theoretical models presented to robustly determine the thickness of the films. SiO_2 is the wavelength-dependent refractive index.

4. Results and Discussion

Through the CE global optimization method, the thickness of the SiO_2 thin film and its respective refractive index were simultaneously fitted. The thickness was obtained by fitting Equation 11 where the input parameters were the refractive indices of the set air/film/substrate Figure 1. As an approximation, the refractive index of air n_2=1 was adopted. The refractive index of the substrate n_0 was calculated using Equation 4 using the reflectance measurement in the silicon reference sample made in the laboratory. On the other hand, n_1 was fitted using the Cauchy Equation 5 defining the coefficients and using the wavelengths at the limit of the spectrometer. With the refractive indices of the media defined, the only free parameter in the multilayer model's reflectance equation is the thickness of the thin film d_1 that was fitted for the six oxidized samples. The results obtained for the three SiO_2 samples that were oxidized using the time of ten hours are presented in Table 1.

Table 1: Sample preparation parameters and results obtained through the fit model for samples oxidized in ten hours.

Samples	Oxidation time(h)	Temperature (°C)	**The film thickness of SiO_2**(nm)
1	10	800	87.9±4.8
2	10	900	277.3±7.1
3	10	1000	404.4±5.8

Source: Authors.

Figure 5 shows the comparison between the reflectance measurement made in the laboratory and the adjustment performed, as well as the refractive index obtained for silicon dioxide. The wavelength range from 328 to 1081.5 nm was used. The thickness obtained through the developed method was 87.9 ± 4.8 nm.

Figure 5: Fit of sample 800 degrees 10 hours. (a) Reflectance and (b) SiO_2 refractive index as a function of wavelength.

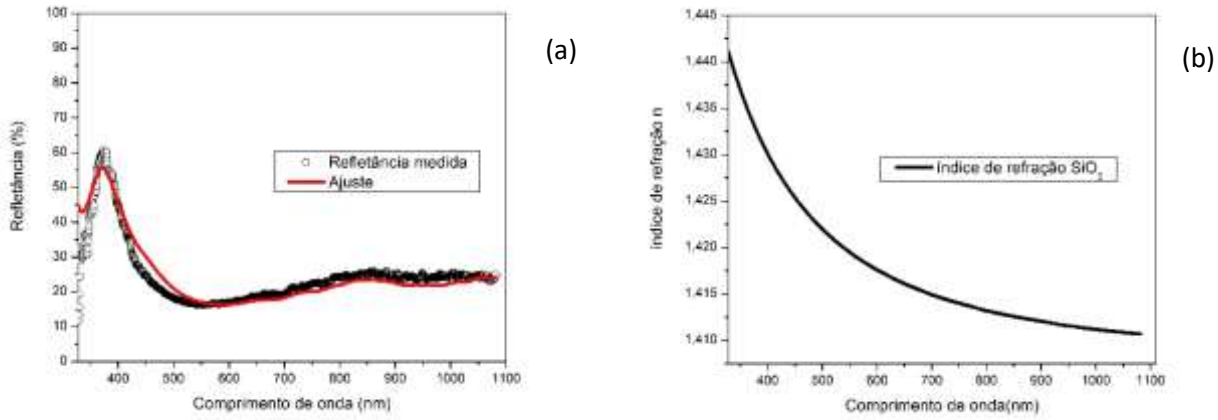

Source: Authors.

The sample is shown in Figures 5(a) and (b) is the thinnest. Its thickness is smaller compared to the wavelength of the incident light, which makes the adjustment more complex. Despite this, the model proved to be efficient in obtaining the expected value for the film. As for the SiO_2 refraction index, shown in Figure 1(b), the obtained value is consistent with the theoretical value.

In the second sample of the ten-hour series, a temperature of 900ºC was used, the Figure 2(a) shows the comparison between the reflectance measurements made in the laboratory and the adjustment performed. It is possible to see that with the rise in temperature, interference patterns that do not exist in Sample 1 appear. This fact shows the dependence of the film thickness on the oxidation temperature and in this case, the obtained thickness was 277.3±7.1 nm. It is observed that the refractive index of Sample 2 (Figure 2}(b)) is higher compared to Sample 1 this can be explained because the obtained value is an average value of the refractive index over the thickness of the film (Huanca & Salcedo, 2015).

Figure 6: Fit of sample 900 degrees 10 hours. (a) Reflectance and (b) SiO_2 refractive index as a function of wavelength.

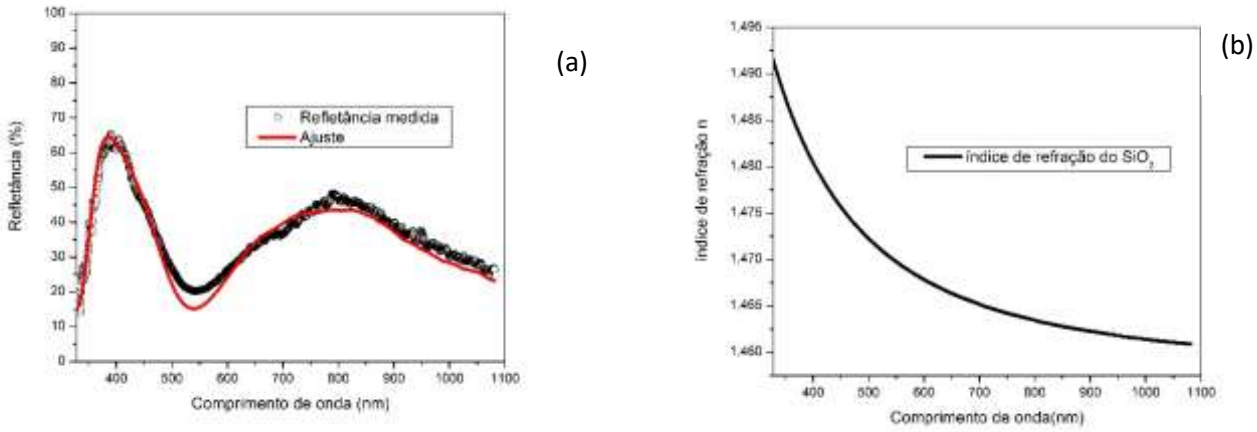

Source: Authors.

Sample 3 was oxidized using a temperature of 1000ºC and a thickness of 404.36±5.84 nm for fine of SiO_2 was obtained. It is observed in Figure 7 the increase in interference patterns is due to the increase in the thickness of the film that was oxidized at a higher temperature. This fact proves the dependence of the thickness on the temperature mentioned in the analysis of Sample 2.

Figure 7: Fit of sample 1000 degrees 10 hours. (a) Reflectance and (b) SiO_2 refractive index as a function of wavelength.

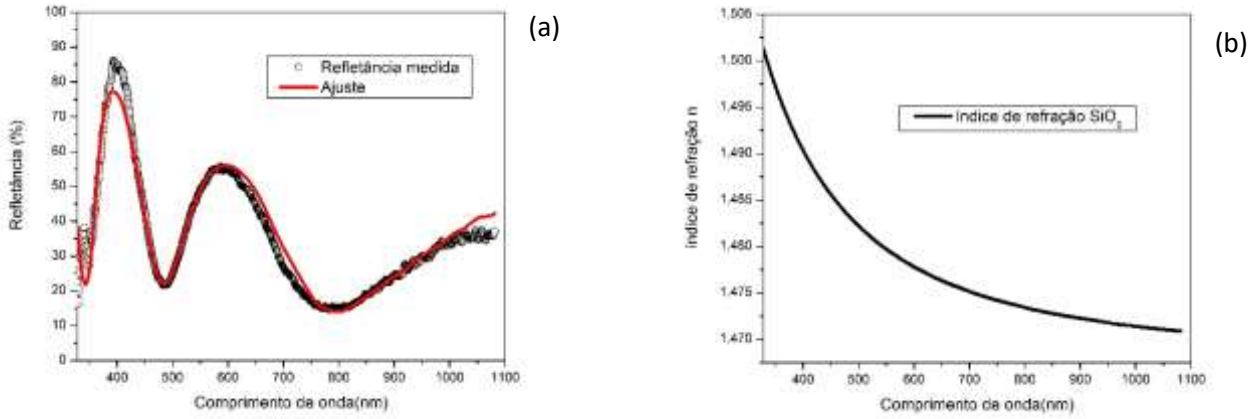

Source: Authors.

Another factor that influences the thickness of the films is the oxidation time. For this reason, the second series of samples with a twelve-hour oven time was prepared. The parameters used in the preparation of this series are presented in Table 2 together with the solutions obtained for the thickness of thin films of silicon dioxide.

Table 2: Sample preparation parameters and results obtained through the fit model for samples oxidized in twelve hours.

Samples	Oxidation time(h)	Temperature (°C)	**The film thickness of SiO_2**(nm)
4	12	800	132.3±7.3
5	12	900	270.9±8.4
6	12	1000	519±13

Source: Authors.

As seen in the table, Sample 4 was oxidized for twelve hours at a temperature of 800ºC. Figure 8 shows the comparison between the adjustment made for reflectance through the global optimization method and the measurement performed in the laboratory.

Figure 8: Fit of sample 800 degrees 12 hours. (a) Reflectance and (b) SiO_2 refractive index as a function of wavelength.

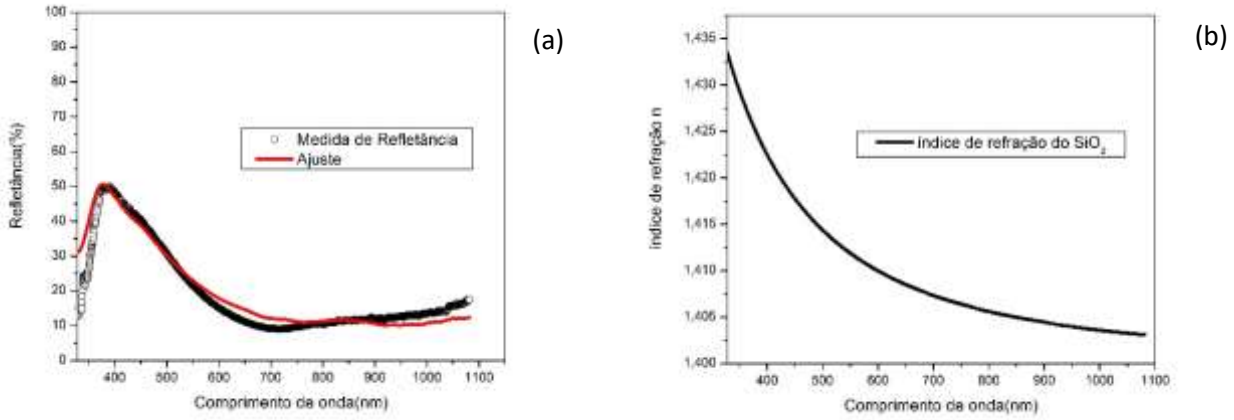

Source: Authors.

With the two-hour increase in oxidation time, the thin film thickness was 132.3±7.2nm. Comparing this value with the value obtained for Sample 1, it is observed that if we vary the oxidation time but keep the same temperature, the thin film thickness changes considerably to the value of 800ºC. Even with the film a little thicker, the adjustment still comes up against the issue of the incident light wavelength value being high when compared to the film thickness. It is also observed that the SiO_2 refractive index has a slightly lower value than that found in Sample 1.

Figure 9 shows the adjustment obtained for Sample 6. This sample presented a peculiar behavior. When comparing the interference pattern obtained in Sample 2 with that obtained in Sample 6, it is observed that they behave similarly. The verification is made through the result of the thin film thickness. The adjustment of the thickness of Sample 5 resulted in the value of 270.9 ±8.4 nm where within the deviation this value equals that obtained for Sample 2.

Figure 9: Fit of sample 900 degrees 12 hours. (a) Reflectance and (b) SiO_2 refractive index as a function of wavelength.

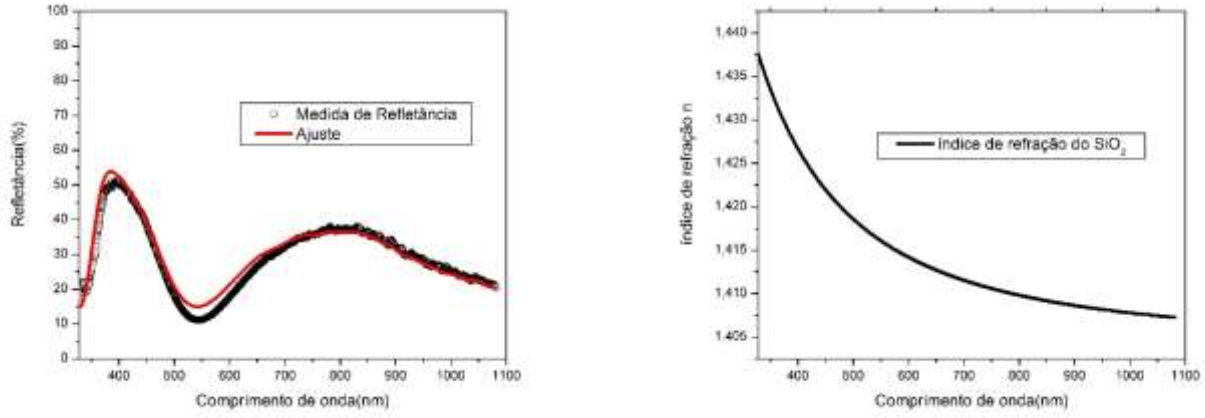

Source: Authors.

This was the sample with the longest oxidation time and the highest temperature. Figure 10 shows the comparison between the experimental and the adjusted reflectance. There is a significant increase in interference patterns when comparing this result obtained with the one obtained for Sample 1.

Figure 10: Fit of sample 1000 degrees 12 hours. (a) Reflectance and (b) SiO_2 refractive index as a function of wavelength.

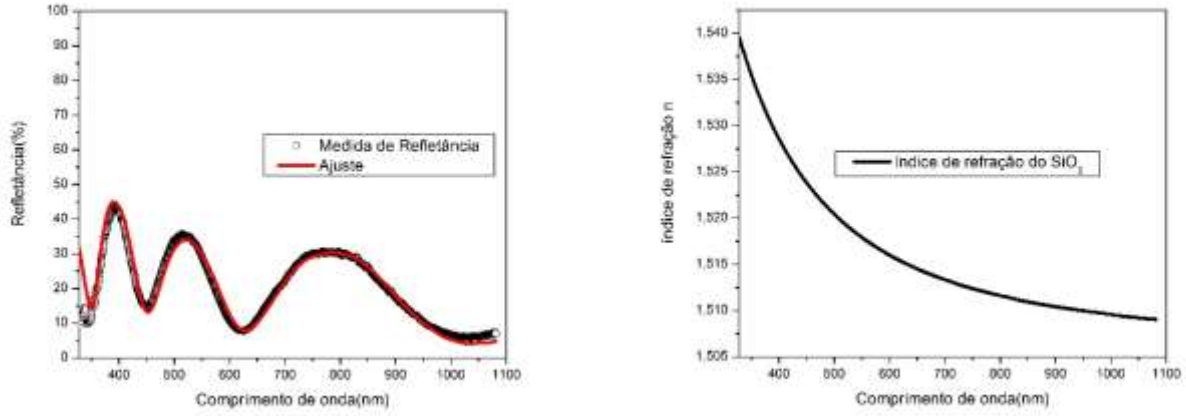

Source: Authors.

Sample 6 showed a better fit of the experimental data, the fit covered the entire experimental curve and the value obtained for the film thickness was 519±13 nm. The SiO_2 refractive index also followed the pattern of increase about samples of this same series as a function of temperature growth, but a decrease to samples of the same temperature in the first series. Such adjustments show that the CE global optimization method is an efficient tool to estimate the thickness of thin films without the need to cut the sample for characterization in a scanning electron microscope.

5. Conclusion

The CE optimization method proved efficient in the adjustments of the reflectance obtained through the measurements carried out in the spectrometer between the wavelengths 328 and 1081.5 nm. The adjustments followed the correct behavior of

the curves for the different thickness variations of the samples. The different curves show the increasing interference patterns according to the increase in the thickness of the silicon dioxide layer on the substrate surface and with the increase of its oxidation time. With the method, it was possible to successfully obtain the same behavior for the different interference patterns of thickness variations. It was also possible to determine through the simultaneous adjustment the respective refractive index of the SiO_2 thin film. The model is a low-cost resource compared to other thin-film determination techniques, making it a viable method.

For the improvement of this work, in the future the results obtained for the thickness of the films with measurements of scanning electron microscopy (SEM) to determine the precision of the generated result. It is also of interest to generalize for the different materials, fitting the refractive index simultaneously with the thickness of the thin film, thus enabling the creation of a reference library.

Acknowledgments

We are grateful for the financial support from Fapemig, Cnpq, and Capes.

References

Batsanov, S. S., Ruchkin, E. D., & Poroshina, I. A. (2016). *Refractive Indices of Solids*. In Springer Briefs in Applied Sciences and Technology. Springer Singapore. https://doi.org/10.1007/978-981-10-0797-2

Black, R. D., Arthur, S. D., Gilmore, R. S., Lewis, N., Hall, E. L., & Lillquist, R. D. (1988). Silicon and silicon dioxide thermal bonding for silicon-on-insulator applications. *Journal of Applied Physics*, 63(8), 2773–2777. https://doi.org/10.1063/1.340976

Boos, D. D. (2003). Introduction to the Bootstrap World. *Statistical Science*, 18(2). https://doi.org/10.1214/ss/1063994971

Chakravarty, S., Teng, M., Safian, R., & Zhuang, L. (2021). Hybrid material integration in silicon photonic integrated circuits. *Journal of Semiconductors*, 42(4), 041303. https://doi.org/10.1088/1674-4926/42/4/041303

Curran, A., Gocalinska, A., Pescaglini, A., Secco, E., Mura, E., Thomas, K., Nagle, R. E., Sheehan, B., Povey, I. M., Pelucchi, E., O'Dwyer, C., Hurley, P. K., & Gity, F. (2021). Structural and Electronic Properties of Polycrystalline InAs Thin Films Deposited on Silicon Dioxide and Glass at Temperatures below 500 °C. *Crystals*, 11(2), 160. https://doi.org/10.3390/cryst11020160

Eckertová, L. (2012). *Physics of Thin Films*. Estados Unidos: Springer US.

El-Bindary, A., Anwar, Z., & El-Shafaie, T. (2021). Effect of silicon dioxide nanoparticles on the assessment of quercetin flavonoid using Rhodamine B Isothiocyanate dye. *Journal of Molecular Liquids*, 323, 114607. https://doi.org/10.1016/j.molliq.2020.114607

Gao, L., Lemarchand, F., & Lequime, M. (2013). Refractive index determination of SiO2 layer in the UV/Vis/NIR range: spectrophotometric reverse engineering on single and bi-layer designs. *Journal Of The European Optical Society - Rapid Publications*, 8. doi:10.2971/jeos.2013.13010

Garcia-Caurel, E., De Martino, A., Gaston, J.-P., & Yan, L. (2013). Application of Spectroscopic Ellipsometry and Mueller Ellipsometry to Optical Characterization. *Applied Spectroscopy*, 67(1), 1–21. https://doi.org/10.1366/12-06883

Heavens, O. S. (1991). *Optical Properties of Thin Solid Films*, Dover Books on Physics Series

Huanca, D. R., & Salcedo, W. J. (2015). Optical characterization of one-dimensional porous silicon photonic crystals with effective refractive index gradient in depth. *Physica Status Solidi (a)*, 212(9), 1975–1983. https://doi.org/10.1002/pssa.201532063

Jain, A. K., Dubes, R. C., & Chen, C.-C. (1987). Bootstrap Techniques for Error Estimation. *IEEE Transactions on Pattern Analysis and Machine Intelligence, PAMI-9*(5), 628–633. https://doi.org/10.1109/tpami.1987.4767957

Jesus, J. J. de, Oliveira, A. F., & Silva, A. P. da. (2021). Espectrômetro digital. Uma proposta de construção de um experimento de Física Moderna para o ensino remoto. *Research, Society and Development*, 10(8), e51410817786. https://doi.org/10.33448/rsd-v10i8.17786

Li, J., & Wu, S.-T. (2004). Extended Cauchy equations for the refractive indices of liquid crystals. *Journal of Applied Physics*, 95(3), 896–901. https://doi.org/10.1063/1.1635971

Liu, S., Deng, Z., Li, J., Wang, J., & Huang, N. (2019). Measurement of the refractive index of whole blood and its components for a continuous spectral region. *Journal of Biomedical Optics*, 24(03), 1. https://doi.org/10.1117/1.jbo.24.3.035003

Losurdo, M., Bergmair, M., Bruno, G., Cattelan, D., Cobet, C., de Martino, A., Fleischer, K., Dohcevic-Mitrovic, Z., Esser, N., Galliet, M., Gajic, R., Hemzal, D., Hingerl, K., Humlicek, J., Ossikovski, R., Popovic, Z. V., & Saxl, O. (2009). Spectroscopic ellipsometry and polarimetry for materials and systems analysis at the nanometer scale: state-of-the-art, potential, and perspectives. *Journal of Nanoparticle Research*, 11(7), 1521–1554. https://doi.org/10.1007/s11051-009-9662-6

Oliveira, A. F., Rubinger, R. M., Monteiro, H., Rubinger, C. P. L., Ribeiro, G. M., & de Oliveira, A. G. (2015). Main scattering mechanisms in InAs/GaAs multi-quantum-well: a new approach by the global optimization method. *Journal of Materials Science*, 51(3), 1333–1343. https://doi.org/10.1007/s10853-015-9451-9

Pereira, A.S., Shitsuka, D. M., Parreira, F. J., Shitsuka, R. (2018) *Metodologia de pesquisa científica*, UFSM

Ribeiro, L. H., Ider, J., Oliveira, A. F., Rubinger, R. M., Rubinger, C. P. L., & de Oliveira, A. G. (2021). Investigation of electronic transport in InAs/GaAs samples. A study using the metaheuristic self-adaptive differential evolution method. Physica B: Condensed Matter, 413293. https://doi.org/10.1016/j.physb.2021.413293

Rubinger, R. M., da Silva, E. R., Pinto, D. Z., Rubinger, C. P. L., Oliveira, A. F., & da Costa Bortoni, E. (2015). Comparative and quantitative analysis of white light-emitting diodes and other lamps used for home illumination. *Optical Engineering*, 54(1), 014104. https://doi.org/10.1117/1.oe.54.1.014104

Rubinstein, R. Y. (1997). Optimization of computer simulation models with rare events. *European Journal of Operational Research*, 99(1), 89–112. https://doi.org/10.1016/s0377-2217(96)00385-2

Rubinstein, R. Y. & Kroese, D. P. (2004) *The Cross-Entropy Method: A Unified Approach to Combinatorial Optimization, Monte-Carlo Simulation and Machine Learning (Information Science and Statistics)*, Springer.

Vidakis, N., Petousis, M., Velidakis, E., Tzounis, L., Mountakis, N., Korlos, A., Fischer-Griffiths, P. E., & Grammatikos, S. (2021). On the Mechanical Response of Silicon Dioxide Nanofiller Concentration on Fused Filament Fabrication 3D Printed Isotactic Polypropylene Nanocomposites. *Polymers*, 13(12), 2029. https://doi.org/10.3390/polym13122029

Zhu, W. (1997). Making Bootstrap Statistical Inferences: A Tutorial. Research Quarterly for Exercise and Sport, 68(1), 44–55. https://doi.org/10.1080/02701367.1997.10608865

Zou, X., Ji, L., Ge, J., Sadoway, D. R., Yu, E. T., & Bard, A. J. (2019). Electrodeposition of crystalline silicon films from silicon dioxide for low-cost photovoltaic applications. *Nature Communications*, 10(1). https://doi.org/10.1038/s41467-019-13065-w